

# GS<sup>2</sup>: Graph-based Spatial Distribution Optimization for Compact 3D Gaussian Splatting

## Supplementary Material

Dataset	k	PSNR $\uparrow$	SSIM $\uparrow$	LPIPS $\downarrow$
T&T	5	24.76	0.84	0.22
	10	<b>24.90</b>	<b>0.85</b>	<b>0.21</b>
	15	24.81	0.84	0.21

Table 6. Quantitative results on the T&T dataset with varying hyperparameter  $k$  settings.

### 6. Implementation Details

GS<sup>2</sup> begins densification in Phase 1, followed by pruning in Phase 2 once densification is complete. During Phase 2, pruning is performed every 100 iterations and stops at 30,000 iterations, at which point the learning rate is reset. During the spatial distribution optimization of the pruned Gaussian points, the learning rate is reset every 15,000 iterations. We adopt Euclidean distance in the GSDO module and set  $k = 10$  according to experimental results, as shown in Tab. 6. We set  $\lambda_1 = 0.2$ ,  $\lambda_2 = 3 \times 10^{-5}$ ,  $\lambda_3 = 4 \times 10^{-4}$ ,  $\lambda_c = 1 \times 10^{-2}$ ,  $\lambda_s = 5 \times 10^{-2}$ ,  $\varepsilon = 0.5$  and  $\lambda_\xi = 0.2$ . All 3DGS experiments [6–8, 13, 18, 20, 25] are conducted using the official code and executed on an RTX 3090 GPU with 24 GB of memory under the same settings. Each method is executed five times, and the optimal result is documented.

### 7. More Analysis

We observed that some blur artifacts are caused by anomalous Gaussian points with excessively high opacity, as shown in Fig. 8. Simply increasing the pruning threshold primarily targets low-opacity points and is insufficient for handling these high-opacity anomalies. As illustrated in Fig. 8, even increasing the pruning threshold by a factor of 10 fails to eliminate the blur artifacts. While the linear term encourages Gaussian points to reduce opacity, it does not adaptively account for the properties of these anomalous points. As shown in Fig. 8, increasing the regularization weight of the linear term by a factor of 10 removes some blur artifacts but compromises scene details and degrades rendering quality. In contrast, higher-order terms dynamically penalize Gaussian points based on their opacity. As demonstrated in Fig. 8, our loss formulation encourages more Gaussian points to reduce opacity while preserving overall rendering quality.

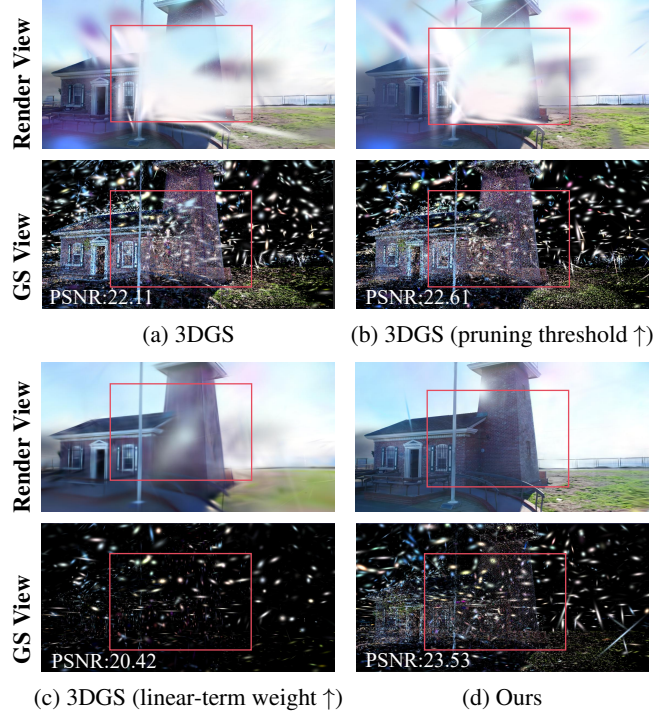


Figure 8. Analysis of the effects of different optimization strategies on anomalous high-opacity Gaussian points.

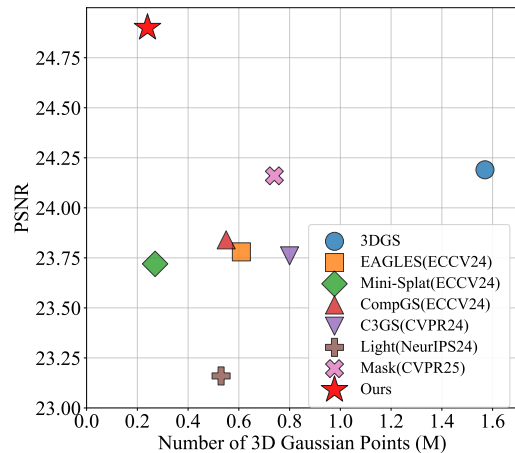


Figure 9. Comparison of rendering quality (PSNR) and number of Gaussian points ( $N_{GS}$ , in millions) for various methods on the Tanks & Temples dataset.

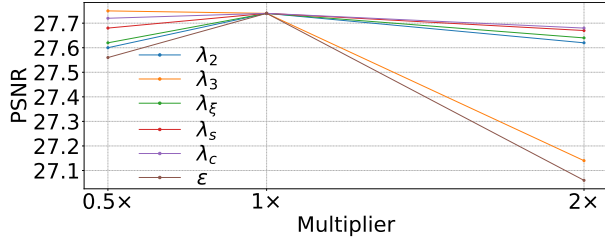


Figure 10. Hyperparameter robustness on Mip-NeRF 360.



Figure 11. Failure cases.

Table 7. Results on LLFF (sparse-view) and T&T (dense-view).

Method	LLFF (PSNR $\uparrow$ / $N_{GS}$ $\downarrow$ )	T&T (PSNR $\uparrow$ / $N_{GS}$ $\downarrow$ )
3DGS-MCMC	22.80 / 0.44	23.75 / 1.48
FDS-GS	<b>25.23</b> / 0.70	23.84 / 1.18
GNS	25.10 / 0.60	<u>24.81</u> / 0.30
Ours	<u>25.16</u> / <b>0.12</b>	<b>24.90</b> / <b>0.24</b>

Table 8. Results on LLFF (sparse-view) and DB (dense-view).

Method	LLFF (PSNR $\uparrow$ / $N_{GS}$ $\downarrow$ )	DB (PSNR $\uparrow$ / $N_{GS}$ $\downarrow$ )
3DGS	<u>25.10</u> / 0.93	29.42 / 2.98
EAGLES	24.27 / 0.50	<u>29.86</u> / 1.19
Mini-Splatting	24.96 / <u>0.23</u>	<b>29.98</b> / <b>0.35</b>
CompGS	24.26 / 0.34	29.76 / 0.56
Compact 3DGS	23.25 / 0.60	29.58 / 1.31
LightGaussian	23.71 / 0.37	27.01 / 0.98
MaskGaussian	24.18 / 0.46	29.69 / 0.70
Ours	<b>25.16</b> / <b>0.12</b>	29.83 / <u>0.45</u>



Figure 12. Qualitative ablation of GSDO.

## 8. Hyperparameter Robustness

We evaluate the robustness of GS<sup>2</sup> with respect to key hyperparameters. Fig. 10 illustrates that the proposed method is stable across most parameter variations.

In particular, performance is relatively insensitive to scaling factors of the majority of hyperparameters, while  $\lambda_3$  and  $\epsilon$  show moderate sensitivity. Overall, GS<sup>2</sup> maintains consistent rendering quality under reasonable parameter perturbations.

## 9. Additional Quantitative Results

Table 7 reports additional quantitative comparisons on LLFF (sparse-view) and Tanks & Temples (dense-view). GS<sup>2</sup> achieves competitive or superior rendering quality while using significantly fewer Gaussian primitives.

On LLFF, GS<sup>2</sup> attains comparable PSNR with substantially reduced model size. On T&T, our method achieves the best PSNR while maintaining strong memory efficiency.

Table 8 further demonstrates that GS<sup>2</sup> generalizes well across datasets using the same hyperparameter configuration.

## 10. Qualitative Ablations of GSDO

Fig. 7 presents qualitative ablations validating the effectiveness of Graph-based Spatial Distribution Optimization (GSDO) and the associated losses  $\mathcal{L}_{\text{cet}}$  and  $\mathcal{L}_{\text{smt}}$ .

Removing GSDO leads to spatially inconsistent Gaussian distributions and increased blur artifacts. The centroid alignment loss  $\mathcal{L}_{\text{cet}}$  improves global spatial coherence, while the smoothness loss  $\mathcal{L}_{\text{smt}}$  enhances local consistency.

## 11. Failure Cases

Saturated regions weaken photometric supervision and reduce reliable gradient signals, which may lead to blur artifacts across different methods. Representative examples are shown in Fig. 11. These cases typically arise in regions with over-exposure or insufficient texture information.

## 12. Dataset licenses

We use the following datasets:

- Mip-NeRF 360 [2]: no license terms provided. Available at <https://jonbarron.info/mipnerf360/>.
- Tanks & Temples [15]: made available under Creative Commons Attribution-NonCommercial-ShareAlike 3.0 License <https://www.tanksandtemples.org/license/>.

## 13. More Experiment Results

Our method outperforms other methods in most scenes from the Tanks & Temples dataset, as shown in Tab. 10, Tab. 11, Tab. 12 and Fig. 9. Most scenes in the Tanks & Temples dataset features prominent architectural structures, whose well-defined geometry facilitates more effective spatial distribution optimization. Additional qualitative results are shown in Fig. 13. We benchmark 3DGS [13], EAGLES [8], Mini-Splatting [7], CompGS [25], Compact3DGS [18], LightGaussian [6], MaskGaussian [20] and our method on the Mip-NeRF 360 [2] and Tanks & Temples datasets [15]; per-scene results are in Tab. 9, Tab. 10, Tab. 11 and Tab. 12.

PSNR $\uparrow$									
	Bicycle	Flowers	Garden	Stump	Treehill	Room	Counter	Kitchen	Bonsai
3DGS	25.63	<b>21.89</b>	<b>27.74</b>	26.90	22.80	31.51	<b>29.12</b>	<b>31.56</b>	32.18
EAGLES	25.47	21.67	27.26	26.92	21.86	31.53	28.39	30.60	31.32
Mini-Splatting	25.22	21.46	26.88	<b>27.24</b>	22.76	31.15	28.38	31.35	31.58
CompGS	25.34	21.58	27.17	26.94	22.92	31.27	28.28	30.64	31.12
Compact 3D Gaussian	25.25	21.34	27.15	26.45	22.88	30.84	28.69	30.60	32.05
LightGaussian	25.54	21.79	27.28	27.04	22.83	30.59	28.66	30.86	31.54
MaskGaussian	<b>25.64</b>	21.81	27.65	26.94	22.85	31.40	29.00	31.06	<b>32.19</b>
Our	25.55	21.73	27.36	27.07	<b>23.35</b>	<b>31.86</b>	29.11	31.51	32.15
SSIM $\uparrow$									
3DGS	<b>0.78</b>	0.62	<b>0.87</b>	0.79	0.65	<b>0.93</b>	<b>0.92</b>	<b>0.93</b>	<b>0.95</b>
EAGLES	0.77	0.61	0.86	0.78	0.62	<b>0.93</b>	0.91	<b>0.93</b>	0.94
Mini-Splatting	0.77	<b>0.63</b>	0.85	<b>0.81</b>	0.65	0.92	0.90	<b>0.93</b>	0.94
CompGS	0.77	0.60	0.86	0.78	0.65	0.92	0.90	0.92	0.94
Compact 3D Gaussian	0.75	0.59	0.85	0.77	0.65	0.92	0.90	0.92	0.94
LightGaussian	0.77	0.61	0.85	0.78	0.65	0.92	0.91	<b>0.93</b>	0.94
MaskGaussian	<b>0.78</b>	0.62	<b>0.87</b>	0.79	0.65	<b>0.93</b>	0.91	<b>0.93</b>	0.94
Our	0.77	0.61	0.85	0.78	<b>0.66</b>	0.92	0.91	<b>0.93</b>	0.94
LPIPS $\downarrow$									
3DGS	<b>0.20</b>	<b>0.33</b>	<b>0.09</b>	0.21	0.32	<b>0.19</b>	<b>0.18</b>	<b>0.11</b>	<b>0.17</b>
EAGLES	0.22	0.35	0.14	0.22	0.40	0.20	0.19	0.12	0.19
Mini-Splatting	0.23	<b>0.33</b>	0.15	<b>0.20</b>	<b>0.31</b>	0.22	0.20	0.13	0.20
CompGS	0.24	0.36	0.14	0.23	0.35	0.21	0.21	0.13	0.20
Compact 3D Gaussian	0.25	0.37	0.14	0.25	0.34	0.20	0.20	0.13	0.19
LightGaussian	0.23	0.36	0.13	0.22	0.35	0.22	0.20	0.13	0.20
MaskGaussian	0.23	0.35	0.13	0.23	0.34	0.22	0.20	0.14	0.20
Our	0.25	0.37	0.15	0.23	0.36	0.21	0.19	0.13	0.19
$N_{GS}\downarrow$									
3DGS	5.81	3.38	5.03	4.61	3.66	1.48	1.17	1.74	1.25
EAGLES	2.07	1.23	1.42	2.16	1.55	0.67	0.56	0.99	0.64
Mini-Splatting	0.53	0.57	0.56	0.61	0.57	0.39	0.41	0.43	0.36
CompGS	1.33	1.05	1.35	1.20	1.00	0.36	0.42	0.61	0.43
Compact 3D Gaussian	2.21	1.48	2.00	1.12	0.51	2.06	0.52	1.67	0.59
LightGaussian	1.80	1.17	1.78	1.67	1.14	0.45	0.43	0.63	0.54
MaskGaussian	2.90	1.75	2.47	2.29	2.02	0.37	0.41	0.78	0.46
Our	<b>0.35</b>	<b>0.48</b>	<b>0.23</b>	<b>0.33</b>	<b>0.23</b>	<b>0.31</b>	<b>0.18</b>	<b>0.43</b>	<b>0.18</b>

Table 9. Per-scene quantitative results from the Mip-NeRF 360.

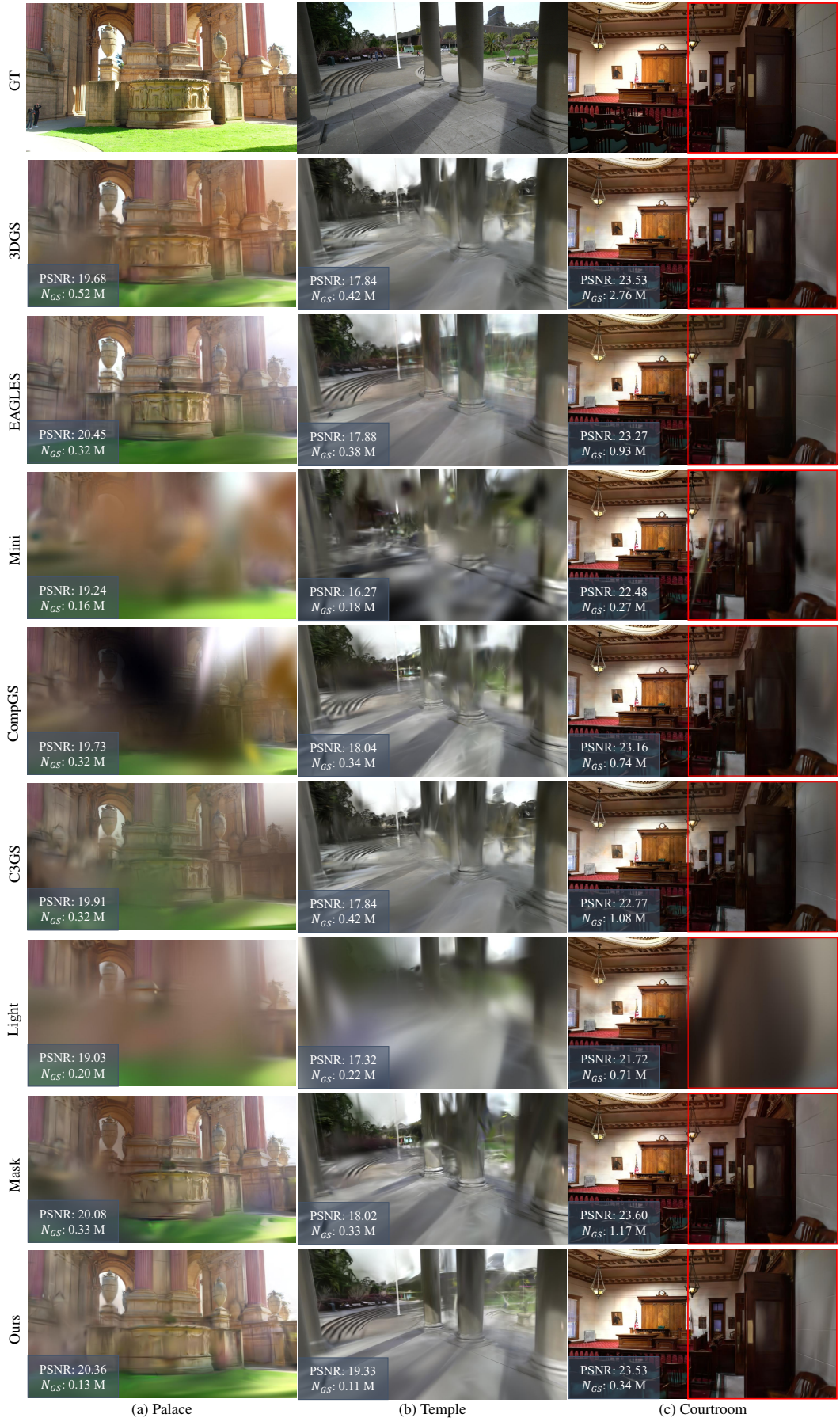


Figure 13. Qualitative comparison on three scenes (*Palace*, *Temple* and *Courtroom*) from the Tanks & Temples dataset. Key regions are enlarged to highlight visual differences. We report the PSNR and  $N_{GS}$  (in millions) for each method.

PSNR $\uparrow$							
	Auditorium	Ballroom	Barn	Caterpillar	Church	Courthouse	Courtroom
3DGS	24.45	25.26	<b>28.48</b>	23.75	23.37	22.43	23.53
EAGLES	23.99	24.97	27.81	23.09	22.78	22.54	23.27
Mini-Splatting	23.73	24.56	28.10	23.39	22.36	21.72	22.48
CompGS	24.28	24.92	27.92	23.14	22.86	21.99	23.16
Compact 3D Gaussian	23.85	24.74	27.67	23.28	22.54	21.86	22.77
LightGaussian	22.91	23.86	27.38	23.22	21.65	21.15	21.72
MaskGaussian	24.42	25.28	28.26	23.73	23.46	22.27	<b>23.60</b>
Ours	<b>25.23</b>	<b>25.43</b>	28.39	<b>24.35</b>	<b>24.10</b>	<b>23.18</b>	23.53
SSIM $\uparrow$							
3DGS	0.88	0.86	0.87	<b>0.81</b>	0.84	0.79	0.81
EAGLES	0.87	0.85	0.86	0.78	0.83	0.79	0.81
Mini-Splatting	0.87	0.84	<b>0.88</b>	0.80	0.82	0.77	0.79
CompGS	0.88	0.85	0.86	0.79	0.83	0.78	0.80
Compact 3D Gaussian	0.87	0.85	0.85	0.78	0.81	0.77	0.79
LightGaussian	0.84	0.82	0.84	0.78	0.78	0.74	0.76
MaskGaussian	0.88	0.86	0.87	0.81	0.84	0.79	0.81
Ours	<b>0.89</b>	<b>0.86</b>	0.86	0.80	<b>0.84</b>	<b>0.79</b>	<b>0.82</b>
LPIPS $\downarrow$							
3DGS	<b>0.22</b>	<b>0.12</b>	0.18	0.21	0.20	<b>0.26</b>	<b>0.19</b>
EAGLES	0.23	0.14	0.21	0.25	0.21	0.26	0.20
Mini-Splatting	0.24	0.15	<b>0.17</b>	0.23	0.23	0.28	0.22
CompGS	0.24	0.14	0.21	0.24	0.22	0.28	0.21
Compact 3D Gaussian	0.24	0.14	0.20	0.25	0.23	0.29	0.22
LightGaussian	0.29	0.18	0.24	0.27	0.29	0.35	0.26
MaskGaussian	0.22	0.12	0.19	<b>0.22</b>	<b>0.20</b>	0.26	0.19
Ours	0.22	0.13	0.21	0.24	0.22	0.27	0.20
$N_{GS}\downarrow$							
3DGS	0.59	2.67	0.75	1.08	1.74	0.29	2.76
EAGLES	0.27	0.95	0.38	0.46	0.82	0.29	0.93
Mini-Splatting	<b>0.08</b>	<b>0.32</b>	0.37	0.29	0.26	0.20	<b>0.27</b>
CompGS	0.31	1.04	0.41	0.57	0.70	0.28	0.74
Compact 3D Gaussian	0.41	1.71	0.57	0.68	1.21	0.33	1.08
LightGaussian	0.18	0.81	0.33	0.44	0.57	0.18	0.71
MaskGaussian	0.26	1.55	0.43	0.67	0.99	0.24	1.17
Ours	0.11	0.41	<b>0.16</b>	<b>0.23</b>	<b>0.25</b>	<b>0.12</b>	0.34

Table 10. Per-scene quantitative results on Tanks & Temples (Part1).

PSNR $\uparrow$							
	Family	Francis	Horse	Ignatius	Lighthouse	M60	Meetingroom
3DGS	25.31	27.77	24.59	22.53	22.11	27.83	25.75
EAGLES	24.93	26.84	23.78	21.54	22.05	27.30	25.18
Mini-Splatting	25.71	28.26	24.95	22.08	21.17	27.57	25.31
CompGS	25.02	27.27	24.12	22.04	21.88	27.36	25.34
Compact 3D Gaussian	25.08	27.93	24.60	22.23	22.16	27.33	24.95
LightGaussian	24.78	26.67	23.72	21.42	21.14	26.92	24.20
MaskGaussian	25.33	27.72	24.31	22.39	22.06	27.78	25.51
Ours	<b>26.43</b>	<b>29.90</b>	<b>25.73</b>	<b>23.81</b>	<b>23.53</b>	<b>28.04</b>	<b>26.48</b>
SSIM $\uparrow$							
3DGS	0.89	0.91	0.90	0.81	0.84	0.90	0.88
EAGLES	0.88	0.90	0.89	0.80	0.84	0.89	0.87
Mini-Splatting	0.89	<b>0.92</b>	0.90	0.81	0.83	0.90	0.88
CompGS	0.89	0.90	0.89	0.80	0.84	0.89	0.88
Compact 3D Gaussian	0.88	0.90	0.89	0.80	0.83	0.89	0.87
LightGaussian	0.88	0.89	0.89	0.79	0.82	0.88	0.85
MaskGaussian	0.89	0.90	0.89	0.81	0.84	0.90	0.87
Ours	<b>0.89</b>	0.91	<b>0.90</b>	<b>0.81</b>	<b>0.84</b>	<b>0.90</b>	<b>0.89</b>
LPIPS $\downarrow$							
3DGS	<b>0.12</b>	<b>0.24</b>	<b>0.13</b>	<b>0.17</b>	<b>0.21</b>	<b>0.15</b>	<b>0.18</b>
EAGLES	0.14	0.25	0.15	0.20	0.22	0.16	0.19
Mini-Splatting	0.13	0.24	0.13	0.20	0.23	0.15	0.20
CompGS	0.14	0.26	0.15	0.19	0.22	0.17	0.20
Compact 3D Gaussian	0.14	0.26	0.15	0.20	0.23	0.17	0.21
LightGaussian	0.14	0.27	0.15	0.21	0.26	0.20	0.23
MaskGaussian	0.12	0.25	0.14	0.17	0.21	0.15	0.19
Ours	0.13	0.25	0.14	0.20	0.22	0.16	0.19
$N_{GS}\downarrow$							
3DGS	2.12	0.72	1.24	3.15	0.67	1.45	1.20
EAGLES	0.83	0.31	0.55	0.96	0.34	0.59	0.47
Mini-Splatting	<b>0.28</b>	0.19	0.24	<b>0.34</b>	0.20	0.35	0.26
CompGS	0.62	0.28	0.40	0.85	0.37	0.53	0.45
Compact 3D Gaussian	0.94	0.30	0.51	1.30	0.42	0.71	0.60
LightGaussian	0.73	0.27	0.49	1.06	0.26	0.53	0.35
MaskGaussian	0.91	0.27	0.51	1.40	0.33	0.62	0.48
Ours	0.35	<b>0.14</b>	<b>0.22</b>	0.40	<b>0.14</b>	<b>0.23</b>	<b>0.22</b>

Table 11. Per-scene quantitative results on Tanks & Temples (Part2).

PSNR↑							
	Museum	Palace	Panther	Playground	Temple	Train	Truck
3DGS	21.34	19.68	28.49	25.78	17.93	22.12	25.43
EAGLES	21.03	<b>20.45</b>	27.98	25.54	17.88	21.46	25.05
Mini-Splatting	21.17	19.24	28.04	25.19	16.27	21.55	25.28
CompGS	21.32	19.73	28.23	25.55	18.04	21.53	24.97
Compact 3D Gaussian	20.19	19.91	28.23	25.30	17.84	21.56	25.02
LightGaussian	19.87	19.03	28.02	25.29	17.32	21.34	24.83
MaskGaussian	21.33	20.08	28.48	26.10	18.02	21.84	25.33
Ours	<b>21.77</b>	20.36	<b>28.79</b>	<b>26.52</b>	<b>19.33</b>	<b>22.51</b>	<b>25.53</b>
SSIM↑							
3DGS	0.79	0.74	0.91	0.86	0.75	0.81	0.88
EAGLES	0.80	<b>0.75</b>	0.91	0.85	0.76	0.80	0.88
Mini-Splatting	0.79	0.72	0.91	0.86	0.70	0.81	0.88
CompGS	0.80	0.73	0.91	0.85	0.75	0.80	0.87
Compact 3D Gaussian	0.78	0.73	0.90	0.84	0.75	0.79	0.87
LightGaussian	0.76	0.71	0.90	0.83	0.73	0.78	0.87
MaskGaussian	0.79	0.74	0.91	0.86	0.75	0.81	0.88
Ours	<b>0.80</b>	0.74	<b>0.91</b>	<b>0.86</b>	<b>0.78</b>	<b>0.81</b>	<b>0.88</b>
LPIPS↓							
3DGS	<b>0.19</b>	<b>0.33</b>	<b>0.14</b>	<b>0.17</b>	0.31	<b>0.21</b>	0.15
EAGLES	0.20	0.33	0.16	0.20	0.31	0.24	0.16
Mini-Splatting	0.22	0.37	0.14	0.19	0.36	0.22	<b>0.14</b>
CompGS	0.20	0.35	0.16	0.20	0.32	0.23	0.17
Compact 3D Gaussian	0.21	0.35	0.16	0.20	0.33	0.24	0.16
LightGaussian	0.23	0.40	0.17	0.23	0.36	0.28	0.17
MaskGaussian	0.19	0.33	0.14	0.17	0.31	0.21	0.15
Ours	0.20	0.34	0.15	0.20	<b>0.30</b>	0.24	0.16
$N_{GS}$ ↓							
3DGS	4.34	0.52	1.71	2.18	0.66	0.70	2.44
EAGLES	1.35	0.32	0.61	0.77	0.38	0.46	0.84
Mini-Splatting	<b>0.33</b>	0.16	0.36	0.32	0.18	0.28	0.32
CompGS	1.01	0.32	0.51	0.73	0.34	0.53	0.60
Compact 3D Gaussian	1.98	0.32	0.75	0.96	0.42	0.71	0.95
LightGaussian	1.28	0.20	0.58	0.73	0.22	0.35	0.91
MaskGaussian	2.00	0.29	0.60	1.40	0.33	0.62	0.89
Ours	0.38	<b>0.13</b>	<b>0.25</b>	<b>0.32</b>	<b>0.11</b>	<b>0.18</b>	<b>0.29</b>

Table 12. Per-scene quantitative results on Tanks & Temples (Part3).